

On the Inflection in the Concentration Dependence of the Maxwell–Stefan Diffusivity of CF₄ in MFI Zeolite

R. Krishna,* J. M. van Baten, and D. Dubbeldam

Van 't Hoff Institute for Molecular Sciences, University of Amsterdam, Nieuwe Achtergracht 166, 1018 WV Amsterdam, The Netherlands

Received: July 31, 2004; In Final Form: August 20, 2004

The recently published data on the Maxwell–Stefan diffusivity \mathfrak{D} of CF₄ in MFI zeolite (*J. Phys. Chem. B* 2004, 108, 10613) shows an inflection at a loading $\Theta = 12$ molecules per unit cell, corresponding to the inflection in the adsorption isotherm. We investigate the underlying reasons by performing kinetic Monte Carlo simulations and show that at $\Theta = 12$, the molecular traffic along the zigzag channels comes to a virtual stand-still and further transport occurs only along the straight channels of MFI. The inflection behavior of \mathfrak{D} is likely to be a generic characteristic of transport in nanoporous materials in which the adsorption of the diffusant occurs on multiple sites with widely different strengths.

In a recent Letter Jobic et al.¹ have reported experimental data on the dependence of the Maxwell–Stefan (M–S) or corrected diffusivity, \mathfrak{D} , for CF₄ in silicalite-1 (MFI zeolite topology) as a function of the molecular loading Θ , expressed in molecules per unit cell, for temperatures $T = 200$ and 250 K. The authors also report good quantitative agreement between the experimental data on \mathfrak{D} and molecular dynamics (MD) simulation results. Generally speaking, the M–S diffusivity decreases with increased loading, in agreement with MD simulation results at 298 K reported earlier by Skoulidas et al.^{2–4} In Figure 1a their MD simulation results for the *normalized* M–S diffusivity $\mathfrak{D}/\mathfrak{D}(0)$ are plotted against Θ for $T = 200$, 250, and 298 K. For all three temperatures $\mathfrak{D}/\mathfrak{D}(0)$ is seen to *decrease* as the loading is increased from $\Theta = 0$ to $\Theta = 12$ and *increase* as the loading is increased further. Jobic et al.¹ also make this observation in their discussions but do not offer a physical explanation for the increase in \mathfrak{D} for $\Theta > 12$. The Fick diffusivity $D = \mathfrak{D}\Gamma$, where Γ is the thermodynamic correction factor $\Gamma \equiv \partial \ln p / \partial \ln \Theta$, is seen to exhibit the opposite trend with a *maximum* at $\Theta = 12$; see Figure 1b. A clue to the inflection behaviors of \mathfrak{D} and D can be found in the adsorption isotherms¹ that show a clear inflection at a loading of $\Theta = 12$; see, for example, the grand canonical Monte Carlo (GCMC) simulation results of the adsorption isotherm at 298 K shown in Figure 1c. The isotherm inflection can be rationalized by the fact that of the total of 16 adsorption “sites”, 4 are to be considered “weak” in that these are only occupied at higher pressures. A dual-site Langmuir model:

$$\Theta(p) \equiv \Theta_A + \Theta_B = \frac{\Theta_{\text{sat,A}} b_A p}{1 + b_A p} + \frac{\Theta_{\text{sat,B}} b_B p}{1 + b_B p}$$

fits the isotherm data perfectly; see continuous lines in Figure 1c, drawn using the parameter values specified in Table 1.

The inflection in the Θ dependence of the Fick diffusivity D has been emphasized earlier by Skoulidas et al.⁴ and follows the trend portrayed by Γ , also shown in Figure 1b by continuous

TABLE 1: Zero-Loading Diffusivities and Dual-Site Langmuir Parameters for CF₄ in MFI at 200, 250, and 298 K and for CH₄ in FAU at 300 K

zeolite	molecule	temp (K)	$\mathfrak{D}(0)$	dual-site Langmuir parameters			
				b_A	$\Theta_{\text{sat,A}}$	b_B	$\Theta_{\text{sat,B}}$
MFI	CF ₄	200	0.2	3.75×10^{-3}	12	1.1×10^{-5}	4
		250	0.32	1.36×10^{-4}	12	3.6×10^{-7}	4
		298	0.47	2.21×10^{-5}	12	5.7×10^{-8}	4
FAU	CH ₄	300	3.5	3.14×10^{-7}	80	2.23×10^{-9}	40

^a The $\mathfrak{D}(0)$ has units of $10^{-8} \text{ m}^2 \text{ s}^{-1}$. The saturation capacity Θ_{sat} has units of molecules per unit cell. The Langmuir parameters, b , have units Pa^{-1} . The data in this table are extracted from the GCMC and MD simulations of Skoulidas et al.^{1–4} and Chempath et al.¹²

dashed lines. In these calculations of Γ the following analytic formula, derived earlier,^{5,6} has been used: $\Gamma = 1/(x_A(1 - \Theta_A/\Theta_{\text{sat,A}}) + x_B(1 - \Theta_B/\Theta_{\text{sat,B}}))$, where $x_A = \Theta_A/(\Theta_A + \Theta_B)$ and $x_B = \Theta_B/(\Theta_A + \Theta_B)$ are the fractions of the total loadings at sites A (channel interiors) and B (intersections).

The inflection in the M–S diffusivity \mathfrak{D} , however, has not been stressed in the published literature. The loading dependence of the M–S diffusivity \mathfrak{D} appears to be dictated by the inverse of the thermodynamic correction factor $1/\Gamma$ that displays a cusp-like inflection at $\Theta = \Theta_{\text{sat,A}}$ (see the continuous dashed lines in Figure 1a). Our objective here is to provide physical insights into the inflection behavior of \mathfrak{D} . We underpin our arguments by performing kinetic Monte Carlo (KMC) simulations of the M–S diffusivity of CF₄ at 298 K following the methodology outlined in earlier publications.^{7–9}

The MFI lattice topology (see Figure 2) is made up of equal sized sorption sites, 16 in total, distributed along the straight channels (4) and zigzag channels (8) and at the intersections (4). The assumed distribution of molecules in the various locations were decided after examination of snapshots of the molecular sitings from our own GCMC simulations at varying pressures. A total of $5 \times 5 \times 5 = 125$ unit cells were simulated. In the KMC simulations we assume that each site can be occupied by only one molecule at a time and there are no further molecule–molecule interactions. Particles can move from one site to a neighboring site via hops. Let ν_{str} and ν_{zz} denote the jump frequencies for movement along the straight and zigzag

* Corresponding author. Fax: + 31 20 5255604. E-mail: R.Krishna@uva.nl.

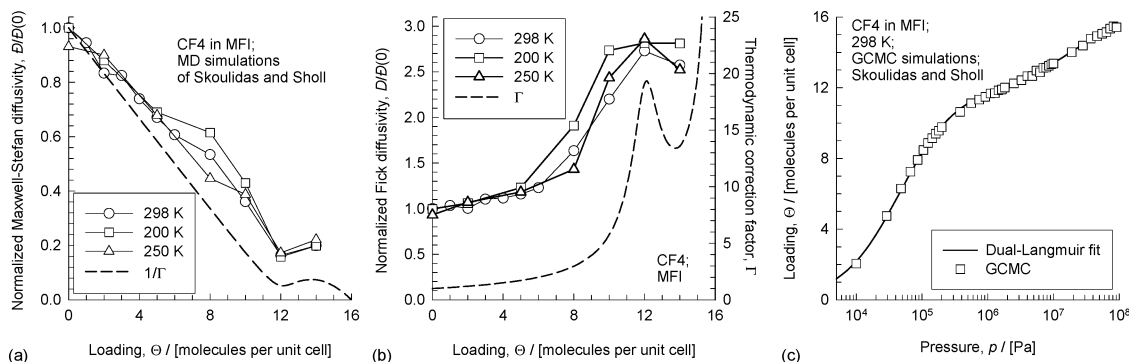


Figure 1. Dependence on the molecular loading, Θ , of (a) the normalized Maxwell–Stefan diffusivity, and (b) the normalized Fick diffusivity for diffusion of CF_4 in MFI at 200, 250, and 298 K. The symbols represent the MD simulation results of Skoulidas et al.^{1–4} The continuous dashed lines in (a) and (b) represent, respectively, $1/\Gamma$ and Γ where Γ is the thermodynamic factor. (c) The adsorption isotherm for CF_4 in MFI at 298 K. The symbols represent the GCMC simulations of Skoulidas et al.^{3,4} The continuous dashed lines represent the dual-Langmuir fit of the isotherm with parameters specified in Table 1.

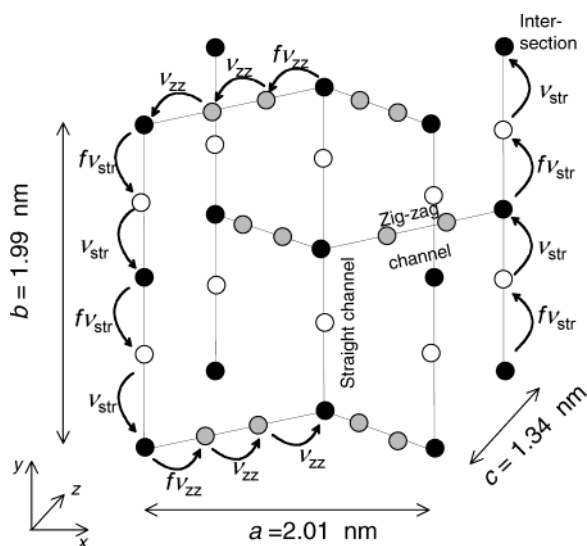


Figure 2. Diffusion unit cell for MFI. Straight and zigzag channels connect at intersections denoted by large black dots. There are two adsorption sites within each of the zigzag channels, denoted by gray dots, and one adsorption site, denoted by white dots, within each straight channel.

channels when moving toward the intersections. The jumps away from the intersections toward either the straight or zigzag channels occur at a frequency, higher by a factor f , because of the preference of CF_4 to locate in the channel interiors. This factor f is determined by the ratio of the Langmuir constants $f = b_A/b_B = 388$; a similar argument was used in our earlier KMC simulations for the diffusion of 2-methylpropane in MFI.^{6,9} The asymmetry in the jump frequencies toward and away from the intersections captures the inflection behavior of the sorption isotherm. This can be verified by KMC simulations of Γ , obtained from fluctuations in molecular jumps using the formula derived by Reed and Ehrlich:¹⁰ $\Gamma = \langle N \rangle / (\langle N^2 \rangle - \langle N \rangle^2)$, where N is the number of sorbed particles in a chosen number of subvolumes of the total simulation box consisting of 125 unit cells. For accurate estimations of Γ we sampled 100 subvolumes. In Figure 3a the Γ obtained from KMC simulations using the Reed–Ehrlich formula are seen to be in excellent agreement with calculations of Γ from the dual-Langmuir fit of the isotherm determined by GCMC simulations. The values of v_{str} and v_{zz} are chosen so as to match the data on the zero-loading M–S diffusivities in the x - and y -directions obtained from MD simulations² (see Figure 2 for specification of the coordinate directions): $\mathfrak{D}_x(0) = 0.41 \times 10^{-8} \text{ m}^2 \text{ s}^{-1}$ and $\mathfrak{D}_y(0)$

$= 0.88 \times 10^{-8} \text{ m}^2 \text{ s}^{-1}$. This yields values of $v_{\text{str}} = 5.25 \times 10^{10}$ and $v_{zz} = 3.4 \times 10^{10} \text{ s}^{-1}$, respectively. With this choice of jump frequencies, the KMC simulated values of \mathfrak{D}_x , \mathfrak{D}_y , and \mathfrak{D}_z show excellent agreement with the corresponding MD simulations over the entire loading range (see Figure 3b). The corresponding spatially averaged values of $\mathfrak{D} = (\mathfrak{D}_x + \mathfrak{D}_y + \mathfrak{D}_z)/3$ are compared in Figure 3c. The KMC simulations show a clear minimum at $\Theta = 12$, and a subsequently rise in value to a maximum at $\Theta = 14$ before eventually reaching vanishingly small values at the saturation loading of $\Theta = 16$. At $\Theta = 12$ all the channel sites are occupied and this makes the molecular traffic along the x - and z -directions come to a virtual standstill; witness the vanishing values of \mathfrak{D}_x and \mathfrak{D}_z for values of $\Theta > 12$ in the KMC simulations shown in Figure 3b. It is, however, to be noted that the MD simulations of \mathfrak{D}_x do not reduce to vanishingly small values for $\Theta > 12$ and the reasons for the differences between the MD and KMC simulations of \mathfrak{D}_x in this loading range are not clear. For loadings $\Theta > 12$ the molecular traffic is almost exclusively along the straight channels, in the y -direction. The relatively fast one-dimensional jumps along the straight channels are the reason for the increase in the \mathfrak{D} beyond $\Theta > 12$. Inevitably, as saturation loading is approached, both the fractional vacancy and the diffusivity reduce to zero.

The loading dependence of \mathfrak{D} for CF_4 is entirely analogous to that obtained from KMC simulations for the diffusion of 2-methylpropane in MFI.^{6,9} In the latter case, however, the inflection in the isotherm, occurring at $\Theta = 4$, is caused by preferential location of the branched alkane at the intersections and the KMC simulations reflect this by taking f to be about 4 orders of magnitude smaller than unity. One consequence of the inflection behavior of \mathfrak{D} is that the activation energy for 2-methylpropane changes abruptly at $\Theta = 4$, as has been experimentally observed by Millot et al.;¹¹ an analogous behavior is found for diffusion of 3-methylpentane^{5,11} in MFI.

On the basis of the insights gained from KMC simulations, we suggest the following expression for the loading dependence of \mathfrak{D} :

$$\mathfrak{D} = \mathfrak{D}(0)x_A(1 - \Theta_A/\Theta_{\text{sat},A}) + \mathfrak{D}_y(0)x_B(1 - \Theta_B/\Theta_{\text{sat},B}) \quad (1)$$

The first term on the right of eq 1, with $\mathfrak{D}(0) = 0.47 \times 10^{-8} \text{ m}^2 \text{ s}^{-1}$ approaches zero at $\Theta = 12$. The second term represents the loading dependence of the transport along the straight channels with the appropriate zero-loading diffusivity $\mathfrak{D}_y(0) = 0.88 \times 10^{-8} \text{ m}^2 \text{ s}^{-1}$, as determined from Figure 3b. Calculations using eq 1 are shown by continuous solid lines in Figure 3c,

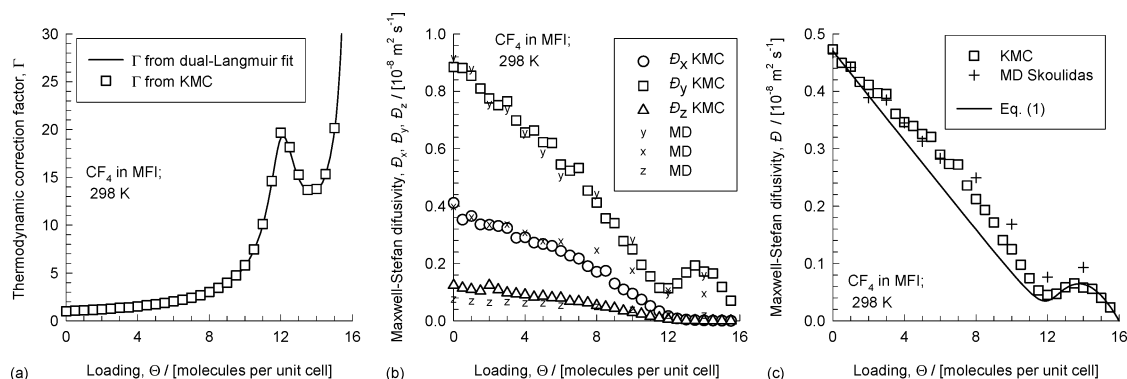


Figure 3. (a) Dependence of the thermodynamic factor Γ as a function of molecular loading Θ for CF_4 in MFI at 298 K. The square symbols represent the results from KMC simulations. The continuous dashed lines represent the calculations of Γ from dual-Langmuir fit of the isotherm with parameters specified in Table 1. (b) Maxwell–Stefan diffusivities in x , y , and z directions as a function of Θ . (c) Spatially averaged Maxwell–Stefan diffusivity of CF_4 in MFI at 298 K as a function of Θ . The open symbols represent KMC simulation results and the cross-hairs are the MD simulation results of Skoulidas et al.^{1–4}

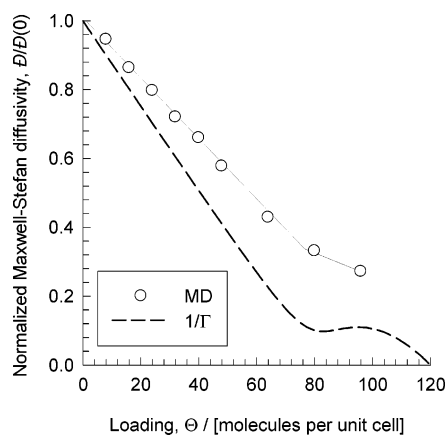


Figure 4. Maxwell–Stefan diffusivity of CH_4 in FAU at 300 K as a function of Θ . The open symbols represent the MD simulation results of Chempath et al.¹² The continuous dashed lines represent $1/\Gamma$, calculated from the dual-Langmuir fit of the GCMC simulated isotherm data with parameters specified in Table 1.

and we see that the MD and KMC simulations follow trend predicted by eq 1 reasonably closely. In the limiting case of a single-site Langmuir isotherm, eq 1 simplifies to yield $\bar{\Delta} = \bar{\Delta}(0)(1 - \Theta/\Theta_{\text{sat}})$, termed the “strong-confinement scenario” by Skoulidas et al.⁴ We agree with the remark made by Jobic et al.¹ that the concept that the M–S diffusivity of CF_4 in MFI follows the strong confinement scenario is too simplistic and offer eq 1 as the appropriate generalization for this case.

We also believe the inflection in the $\bar{\Delta} - \Theta$ dependence observed for CF_4 diffusion in MFI is of a generic nature and characteristic for diffusion of molecules in nanoporous materials that show strong inflection in the isotherms. Recent MD

simulations of Chempath et al.¹² for diffusion of CH_4 in FAU zeolite show an inflection, albeit slight, in the $\bar{\Delta} - \Theta$ dependence at $\Theta = 80$ molecules per unit cell; see Figure 4. This inflection in the $\bar{\Delta}$ coincides with isotherm inflection, as evidenced by the calculations of $1/\Gamma$ also shown in Figure 4. For diffusion of N_2 in single walled carbon nanotubes, the MD simulations of Arora et al.¹³ have shown different dependences of the *self*-diffusivity on Θ occur below and above the isotherm inflection, signifying transition from mono- to bilayer adsorption.

Acknowledgment. R.K. acknowledges two grants: *programmasubsidie* and *TOP subsidie* from The Netherlands Foundation for Scientific Research (NWO-CW) for the development of novel concepts in reactive separations technology and for intensification of reactors. R.K. also acknowledges Drs. Sholl and Skoulidas for providing the GCMC and MD data shown in Figures 1c and 3a in Excel format for re-plotting purposes.

References and Notes

- (1) Jobic, H.; Skoulidas, A. I.; Sholl, D. S. *J. Phys. Chem. B* **2004**, *108*, 10613.
- (2) Skoulidas, A. I.; Sholl, D. S. *J. Phys. Chem. B* **2001**, *105*, 3151.
- (3) Skoulidas, A. I.; Sholl, D. S. *J. Phys. Chem. B* **2002**, *106*, 5058.
- (4) Skoulidas, A. I.; Sholl, D. S.; Krishna, R. *Langmuir* **2003**, *19*, 7977.
- (5) Krishna, R.; Baur, R. *Sep. Purif. Technol.* **2003**, *33*, 213.
- (6) Krishna, R.; Paschek, D. *Chem. Eng. J.* **2002**, *85*, 7.
- (7) Paschek, D.; Krishna, R. *Phys. Chem. Chem. Phys.* **2000**, *2*, 2389.
- (8) Paschek, D.; Krishna, R. *Langmuir* **2001**, *17*, 247.
- (9) Paschek, D.; Krishna, R. *Chem. Phys. Lett.* **2001**, *342*, 148.
- (10) Reed, D. A.; Ehrlich, G. *Surf. Sci.* **1981**, *102*, 588.
- (11) Millot, B.; Methivier, A.; Jobic, H.; Moueddeb, H.; Dalmon, J. A. *Microporous Mesoporous Mater.* **2000**, *38*, 85.
- (12) Chempath, S.; Krishna, R.; Snurr, R. Q. *J. Phys. Chem. B* **2004**, *108*, 13481.
- (13) Arora, G.; Wagner, N. J.; Sandler, S. I. *Langmuir* **2004**, *20*, 6268.